

# Further Advances on Discrete Electromechanical Oscillation Control

Sebastian Martinez-Lizana, Héctor Pulgar-Painemal  
Department of Electrical Engineering and Computer Science  
University of Tennessee, Knoxville, TN, 37996  
smartl18@vols.utk.edu, hpulgar@utk.edu

**Abstract**—This paper presents further advances on a novel power system oscillation control based on step-wise changes in power output of electronically-interfaced resources (EIR). This discrete control technique is used to significantly reduce the amplitude of multiple modes in large-scale systems. The mathematical formulation of the discrete electromechanical oscillation control (DEOC) is presented, including the determination of the required discrete power injection/absorption, and optimal switching conditions. Time-domain simulations in a 9-bus and a 39-bus systems validate the effectiveness of the proposed control. Through DEOC, emerging power technologies can actively participate in the power system level control, recognizing their technical limitations. Thereby, the system dynamic response is substantially improved regarding electromechanical oscillations, and new effective controllers are incorporated into the grid.

**Index Terms**—inter-area oscillations, oscillation damping, discrete control, power system control, power system stability.

## I. INTRODUCTION

Global environmental concern all over the world has led to prioritizing renewable, carbon-free sources of energy over conventional generation. Therefore, electrical power systems have been progressively uptaking renewable generation with increasing penetration from non-conventional renewable energy (NCRE), such as wind and solar [1]. This transition, although desirable, has technical consequences in the operation of the electrical grid. A relative reduction of system inertia and intrinsic variability of NCRE may cause larger and more frequent frequency deviations [2] and recurrent electromechanical oscillations. Particularly, local and inter-area oscillations are recognized to become more critical to control in order to guarantee system reliability and resiliency [3].

Power system stabilizers (PSSs) are deployed to improve oscillation damping by adding a supplementary signal to the excitation systems of selected synchronous generators (SGs). However, these PSSs are not always suitable to handle multiple modes of oscillation [4], situation that may be worsened in the upcoming power grid due to features that can ease the appearances of multiple oscillations [5]. Nowadays, the massive deployment of phasor measurement units and the existence of EIRs such as wind turbine generators, utility-scale

This material is based upon work supported by the National Science Foundation under NSF CAREER Grant No. 2044629. This work also made use of shared facilities supported by the Engineering Research Center Program of the National Science Foundation and the Department of Energy under NSF Award No. EEC-1041877 and the CURENT Industry Partnership Program.

PV plants, flexible a.c. transmission systems, high voltage d.c. lines, controlled loads or energy storage systems (ESS) can be exploited to tackle electromechanical oscillation problems [6], [7]. Unfortunately, existing solutions for enabling wind farms and solar power for damping control require power curtailment, leading to under-utilization of available energy potential, and undesired high cost of operation of NCRE. In addition, the installed capacity of ESS such as batteries and flywheels is not yet significant in most grids to be used for damping control purposes.

The design of new control systems and the expansion of the grid control capabilities have been identified as key goals towards developing a highly renewable power grid [8], [9]. Discrete-bang-bang type-control approaches to handle oscillations have been proposed in the past. Yet, these research efforts are based on oversimplified equivalents [10], [11] that are not suitable for large-scale applications, and assume a unique mode of oscillation that is favorably controlled by a controllable component right in the oscillation path [12]–[14]. These fundamental considerations have made these works inapplicable to real systems. Recently, a new approach to discrete control has been proposed [15]. This discrete control approach is promising since it aims to enable emerging power technologies for dynamic control actions while taking into account their particular limitations. In this way, the grid can gain a large number of new effective controllers that have been excluded due to their limited or no control capabilities under continuous control schemes.

This paper presents important advances in oscillation control based on discrete actions of emerging power technologies, such as EIRs. These elements are considered to work on top of traditional oscillation damping controllers. The DEOC acts upon the system through multiple controllable components (CCs) and is able to handle large-scale systems with multiple excited oscillation modes. In order to do so, a momentary shifting of the system equilibrium point is performed at specific switching times that are computed using a switching function and the system's oscillating energy [16]. The remainder of this paper is structured as follows. Section II provides the theoretical development of the DEOC including the general formulation of the problem, determination of discrete power injection by CCs, and switching conditions. Section III presents the study cases to validate the control performance. Conclusions are presented in Section IV.

978-1-6654-9921-7/22/\$31.00 ©2022 IEEE

## II. DISCRETE ELECTROMECHANICAL OSCILLATION CONTROL (DEOC)

The essence of the DEOC is to enable discrete control mechanisms that inject/absorb active power at a given set of buses. This set corresponds to buses whose connected elements (EIRs) can step-wisely adjust their power output, such as energy storage systems, PV solar generation, and wind turbines. To lay the DEOC foundations for a general formulation, for now, a linear model is considered.

### A. General formulation

Consider  $m$  CCs with their active power output given by  $P_{ref} = P_{ref}^0 + \Delta P (\mu_{t_{on}} - \mu_{t_{off}})$ , with  $P_{ref}, P_{ref}^0, \Delta P \in \mathbb{R}^m$ .  $P_{ref}^0$  is the initial power set-point vector,  $\Delta P$  is a vector that contains a predefined quantity for every CC, and must be determined based on both the particular characteristic of the system under study and the number of CCs,  $\mu_\tau = 1, \forall t > \tau$  is the unit step function, and  $t_{on}$ , and  $t_{off}$  the switching times with  $t_{off} > t_{on}$ . Now, consider a system with  $n_g$  SGs represented by a classical model, and the dc load flow formulation to represent the grid of  $n_b$  buses. By eliminating algebraic variables, the model system becomes:

$$\begin{aligned} \begin{bmatrix} \dot{\delta} \\ \dot{\omega} \end{bmatrix} &= \begin{bmatrix} 0 & \omega_s I_{n_g} \\ -\frac{1}{2} H^{-1} B_a & 0 \end{bmatrix} \begin{bmatrix} \delta \\ \omega \end{bmatrix} \\ &+ \begin{bmatrix} \omega_s \mathbf{1}_{n_g} \\ \frac{1}{2} H^{-1} (P_m + B_b P_L - B_c P_{ref}) \end{bmatrix} \end{aligned} \quad (1)$$

for more details refer to [15]. By inspection, the state matrix  $A_{sys}$  has purely imaginary eigenvalues, then the system behaves as an undamped multidimensional harmonic oscillator. Note that  $P_{ref}$  depends on  $\Delta P$ ,  $t_{on}$ , and  $t_{off}$ . If  $t < t_{on}$  or  $t > t_{off}$ , the system equilibrium point is defined as  $x_e = [\delta_e \ \omega_e]^T$ , with  $\delta_e = B_a^{-1} (P_m + B_b P_L - B_c P_{ref}^0)$ , and  $\omega_e = \mathbf{1}_{n_g}$ . Otherwise, the equilibrium point is shifted to  $x_{ce} = [\delta_{ce} \ \omega_{ce}]^T$  ( $ce$ : controlled equilibrium), with  $\delta_{ce} = \delta_e - B_a^{-1} B_c \Delta P$ , and  $\omega_{ce} = \omega_e = \mathbf{1}_{n_g}$ .

Initially, the system is considered to be in steady-state at the equilibrium point  $x_e$ , but the state variables are shifted away from the equilibrium because of a short-circuit. At time  $t_0$  the short-circuit is cleared and the states at that time are  $x(t_0) = x_0$ . A similarity transformation is used to determine the time evolution of the state variables and its derivative  $\forall t \in [t_0, t_{on}]$ , given by:

$$x(t) = V e^{\Lambda(t-t_0)} V^{-1} (x_0 - x_e) + x_e \quad (2)$$

$$\dot{x}(t) = V \Lambda e^{\Lambda(t-t_0)} V^{-1} (x_0 - x_e) \quad (3)$$

where  $V = [v_1, v_2, \dots, v_n]$  is the full rank matrix of right-eigenvectors, each eigenvector  $v_i$  is associated with its corresponding eigenvalue  $\lambda_i$ ,  $\Lambda = V^{-1} A_{sys} V$  is a diagonal matrix that contains all distinct and different to zero eigenvalues, i.e.,  $\Lambda = \text{diag}\{\lambda_1, \lambda_2, \dots, \lambda_n\}$ , and  $n$  is the total number of states, which in this case is  $n = 2n_g$ .

As shown in Fig. 1-(a), after the short-circuit, the system will exhibit a periodic trajectory (black dashed line) centered at

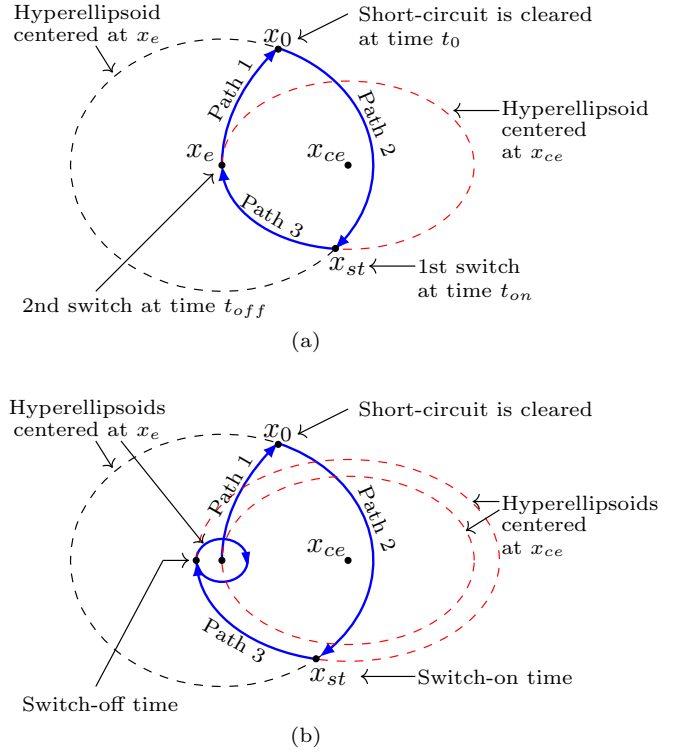


Fig. 1. Graphical description of system trajectories with DEOC: (a) optimal solution, (b) sub-optimal solution.

$x_e$ . The DEOC is activated at some point along the trajectory when  $x(t = t_{st}) = x_{st}$  ( $st$ : switching time), and the system will shift its trajectory to another periodic orbit centered at the controlled equilibrium point  $x_{ce}$ —described by the red dashed line in Fig 1. In the optimal case,  $x_e$  belongs to the controlled periodic orbit, then  $t_{off}$  is set to  $t$  when  $x(t) = x_e$ . The entire DEOC operation will lead the system through the blue trajectory, ultimately eliminating the oscillation. Fig. 1-(b) shows a case when the switch-on is performed slightly after  $x(t) = x_{st}$ . In this case,  $x_e$  would not belong to the controlled periodic trajectory and the oscillation cannot be annihilated. If the switching is not performed at the optimal time, a sub-optimal trajectory near the equilibrium point  $x_e$  will be desirable. In this case, an appropriate way to define the switch-off time is needed (described in subsection II-C).

### B. Power injection from controllable components

The state of the system, right after the disturbance is cleared, will lead to the excitation of the system modes. These will be excited with different intensities depending on both their participation factors  $p_{ki} = w_{ik} v_{ik}$  and the initial condition itself. The explicit solution for the  $k$ -th state variable  $\forall t \in [t_0, t_{on}]$ , this is before the first discrete action, is written as:

$$x_k(t) = \sum_{i=1}^n e^{\lambda_i(t-t_0)} w_i^T (x_0(k) - x_e(k)) v_{ik} \quad (4)$$

where  $w_i^T$ ,  $v_i \in \mathbb{R}^n$  are the  $i$ -th left and right eigenvectors related to the eigenvalue  $\lambda_i$ .

Considering that each SG is described by a classical model, a power system with  $n_g$  synchronous generators (including one at the infinite bus) will have  $n = 2(n_g - 1)$  state variables. These states will exhibit only a few dominant modes in their dynamic response. The main goal of the DEOC is to annihilate the oscillations associated with those modes, thus significantly reducing the amplitude of the oscillatory response. Along these lines, one possible solution to tackle multi-mode systems is presented. This solution pursues oscillation annihilation by progressively targeting one mode at a time.

Without loss of generality, let us assume the oscillation of the  $k$ -th mode is targeted for elimination. For that particular mode one can define the projection  $P = MM^T \in \mathbb{R}^{n \times n}$  over the subspace  $\text{span}\{q_1, q_2\} \in \mathbb{R}^{n \times 2}$ , with  $M = [q_1 \ q_2]$ . Here,  $q_1 = \text{Re}(v_k)$  and  $q_2 = \text{Im}(v_k)$  are the basis of the 2-dimensional projected space, with  $v_k$  being the  $k$ -th eigenvector corresponding to the eigenvalue  $\lambda_k$ . The projection of a vector  $x \in \mathbb{R}^n$  over  $\text{span}\{q_1, q_2\}$  is given by  $Px$ . Now, the representation of the projected vector in the subspace spanned by  $\{q_1, q_2\}$  is determined as:

$$\alpha = \overbrace{(M^T M)^{-1} M^T}^S \underbrace{MM^T}_P x \quad (5)$$

The linear transformation  $S : \mathbb{R}^n \rightarrow \mathbb{R}^2$  can be decomposed into two block matrices  $S = [S_1 \ S_2]$  with proper dimensions, since  $x = [\delta \ \omega]^T$ . In a similar fashion, an orthogonal subspace to  $\text{span}\{q_1, q_2\}$  is defined as:  $N = \text{Null}(M) = \{y \in N \mid My = 0\}$ ,  $N \in \mathbb{R}^{n \times (n-2)}$ . The projector over the null space of  $M$  is given by  $P_n = NN^T$ . The projected vector is  $P_n x$ , and its representation over the projected subspace corresponds to:

$$\alpha_n = \overbrace{(N^T N)^{-1} N^T}^{S_n} \underbrace{NN^T}_{P_n} x \quad (6)$$

Similarly, the linear transformation  $S_n : \mathbb{R}^n \rightarrow \mathbb{R}^{(n-2)}$  can be separated into two block matrices  $S_n = [S_{n1} \ S_{n2}]$  with proper dimensions, since  $x = [\delta \ \omega]^T$ . The orthogonal projections  $P$  and  $P_n$  are very useful to target one mode at a time without exciting others due to the shifting of the equilibrium point. As shown in Fig. 2, to annihilate the oscillation of the dominant mode, the DEOD will affect the equilibrium point over  $\text{span}\{q_1, q_2\}$  and there will be no displacement over the null space of  $M$ . This means that the projected orbits related to any mode but the targeted  $k$ -th mode will have no shifting in the equilibrium point due to the DEOC.

Determining the power injection by each CC to achieve a desired shift of the equilibrium point is a static problem that does not depend on the dynamic trajectory of the system. Due to this, the dc load flow formulation is considered as follows:

$$\begin{bmatrix} \theta \\ \delta \end{bmatrix} = \underbrace{\begin{bmatrix} X_{11} & X_{12} \\ X_{21} & X_{22} \end{bmatrix}}_{B_0^{-1}} \begin{bmatrix} -P_L + A\Delta P \\ P_G \end{bmatrix} \quad (7)$$

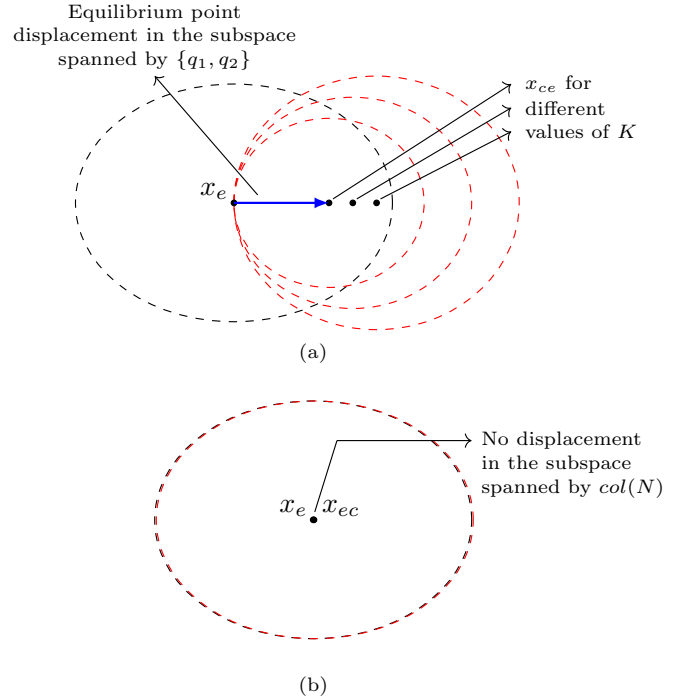


Fig. 2. Graphical description of the representation over the projected subspaces: (a)  $\text{span}\{q_1, q_2\} \in \mathbb{R}^2$ , and (b)  $\text{span}\{\text{col}(N)\} \in \mathbb{R}^{n-2}$ .

where  $\theta \in \mathbb{R}^{n_b}$  in radians are the bus voltage angles,  $B_0 \in \mathbb{R}^{n_g + n_b}$  is the system susceptance matrix including generator's series transient reactance,  $X_{11}, X_{12}, X_{21}, X_{22}$  are the block partitions of  $B_0^{-1}$  with proper dimensions,  $A \in \mathbb{R}^{n_b \times m}$  is an incidence matrix composed of zeros and ones to adjust the size of  $\Delta P$ , such that  $A\Delta P \in \mathbb{R}^{n_b - n_g}$ , by setting zero to entries related to buses where CCs are not connected, and  $P_G \in \mathbb{R}^{n_g}$  is the SG injection power vector. Both the original and controlled equilibrium points are composed of SG loading angle and speed as follows:  $x_e = [\delta_e \ \omega_e]^T$ , and  $x_{ce} = [\delta_{ce} \ \omega_{ce}]^T = [\delta_e + \Delta\delta \ \omega_e]^T$ . Here  $\Delta\delta$  represents the shifting of the equilibrium point with respect to the original.

Following (5) and (6), the projected displacement of the equilibrium point onto  $\text{span}\{q_1, q_2\}$  and its orthogonal subspace are given by  $\Delta\alpha = S_1\Delta\delta$  and  $\Delta\alpha_n = S_{n1}\Delta\delta$ , respectively. Impose a sufficient condition to have zero displacement onto the null space of  $M$ :  $\alpha_n = 0 = S_{n1}\Delta\delta$ . By solving for  $\Delta\delta$ , the required controlled equilibrium point  $x_{ce}$  is defined. This solution is given by:

$$\Delta\delta = K\bar{d} \in \text{Null}(S_{n1}) : |\bar{d}| = 1 \quad (8)$$

where  $K$  is a constant real parameter, and  $\bar{d}$  is the unit direction vector of displacement of the equilibrium point to ensure  $\alpha_n = 0$ . As shown in Fig. 2-(a), different values of  $K$  will lead to different orbits around the controlled equilibrium  $x_{ce}$ . A proper value of  $K$  should be defined, depending on the system, to avoid excessive amplitude of the controlled orbit.

Replacing  $\Delta\delta$  into eq. (7), and solving for  $\Delta P$ , leads to:

$$A\Delta P = X_{21}^+(\delta_c - X_{22}P_G) + P_L \quad (9)$$

where  $X_{21}^+$  is the pseudo-inverse of the block matrix  $X_{21}$ . With this specific power injection  $\Delta P$ , the equilibrium point is only displaced on the representation over the projected subspace  $\text{span}\{q_1, q_2\}$ . It is important to mention that once the oscillation of the targeted dominant mode has been annihilated through DEOC, the process can be repeated to shift the equilibrium point on the representation over the projected subspace  $\text{span}\{q_1, q_2\}$ —now related to the second dominant mode and so on.

### C. Switching conditions

Given the states  $x_0$  right after a short circuit is cleared, the dynamic evolution of the system is defined by equations (2) and (3). Rearrange the equations as follows:

$$V^{-1}(x - x_e) = e^{\Lambda(t-t_0)}V^{-1}(x_0 - x_e) \quad (10)$$

$$\Lambda^{-1}V^{-1}\dot{x} = e^{\Lambda(t-t_0)}V^{-1}(x_0 - x_e) \quad (11)$$

By pre-multiplying eq. (10) by  $(x - x_e)^T(V^{-1})^*$  and eq. (11) by  $\dot{x}^T(V^{-1})^*(\Lambda^{-1})^*$ , and adding them up, lead to an hyper-ellipsoid in the plane  $x - \dot{x}$ :

$$(x - x_e)^T D(x - x_e) + \dot{x}^T E \dot{x} = 2\Delta x_0^T D \Delta x_0 \quad (12)$$

where  $D = (M^{-1})^*M^{-1}$ ,  $E = (M^{-1})^*(\Lambda^{-1})^*\Lambda^{-1}M^{-1}$ ,  $\Delta x_0 = x_0 - x_e$ , and the symbol  $*$  corresponds to the conjugate transpose. Note that  $D$  and  $E$  are real positive definite matrices. This hyper-ellipsoid defines the periodic orbit around the equilibrium point  $x_e$  due to the initial condition  $x_0$ . To successfully apply the DEOC,  $\Delta P$  need to be switched-on at an specific time  $t_{st}$ . In the same way, at  $t_{off} > t_{st}$  the controlled elements are switched back to zero, eliminating the oscillation related to the targeted mode if performed at the optimal time. Consequently, appropriate ways to determine these specific switching times need to be defined.

1) *Switch-on time*: Consider that the states are  $x(t_{st}) = x_{st}$ , right after  $\Delta P$  is discretely switched on. The dynamic trajectory of the system is given by:

$$x(t) = V e^{\Lambda(t-t_{st})} V^{-1}(x_{st} - x_{ce}) + x_{ce} \quad (13)$$

$$\dot{x}(t) = V \Lambda e^{\Lambda(t-t_{st})} V^{-1}(x_{st} - x_{ce}) \quad (14)$$

Rearranging and manipulating the equations in the same fashion as in (10)-(12), lead to another hyper-ellipsoid centered at  $x_{ce}$ , that describes the system trajectory in the plane  $x - \dot{x}$ :

$$(x - x_{ce})^T D(x - x_{ce}) + \dot{x}^T E \dot{x} = 2\Delta x_{st}^T D \Delta x_{st} \quad (15)$$

where  $\Delta x_{st} = x_{st} - x_{ce}$ . To ensure a successful controlled operation, the switch-on should be performed only when  $x_e$  belongs to the controlled trajectory. Thus, using equation (15) and setting  $x = x_e$ , and  $\dot{x}|_{x=x_e} = A(x_e - x_{ce})$ , lead to:

$$\Delta x_{ce}^T (D + A^T E A) \Delta x_{ce} = 2\Delta x_{st}^T D \Delta x_{st} \quad (16)$$

where  $\Delta x_{ce} = x_e - x_{ce}$ . Whenever  $x = x_{st}$  satisfies equation (16),  $\Delta P$  should be switched on. Therefore, the following switching function:

$$h(x) = 2(x_e - x_{ce})^T D(x_e - x_{ce}) - (x - x_{ce})^T (D + A_{sys}^T E A_{sys})(x - x_{ce}) \in \mathbb{R} \quad (17)$$

can effectively determine the switching time when  $h(x) = 0$ .

2) *Switch-off time*: An energy-based approach is used to ensure that the switch back to the equilibrium point  $x_e$  is done appropriately. The oscillation energy is defined as the summation of the individual kinetic energy of the SGs:

$$E_k(t) = \sum_{j=1}^{n_g} H_j \omega_s \Delta \omega_j^2 \quad (18)$$

where  $\Delta \omega_j$  is the speed deviation of SG  $j$  in p.u., and  $H_j$  is the inertia constant of SG  $j$  in s. Note that after a disturbance, the speed trajectories describe the oscillation energy defined by equation (18) such that  $E_k(t) > 0, \forall t > t_0$ . If damping is neglected,  $E_k$  oscillates permanently. The switch-off time  $t_{off}$  should be computed such that  $E_k$  is minimum. This guarantees that the oscillation in the state variables will be close to the equilibrium point—hence the oscillation amplitude is considerably reduced. If performed at the optimal time, the switch-off is performed exactly at the original equilibrium point, thus completely annihilating the targeted oscillation.

For determining the switch-off time, the integral of  $E_k(t)$ —also defined as action [16]—over a moving time window  $[t_1, t_1 + T]$  is determined. Whenever the integral is minimum, the system is reaching a minimum oscillating energy  $E_k$ , and it is the moment to switch-off. This integral needs to be computed for each  $t_1 > t_{st}$  after the switch-on time. Also, an appropriate time window  $T$  needs to be considered to capture the oscillating energy dynamics.

## III. SIMULATION RESULTS AND ANALYSIS

Simulations are performed in a 9-bus system and a 39-bus system [17]. Grid parameters are obtained from the MATPOWER library [18]. No additional controllers are contemplated to evaluate the sole action of the proposed DEOC. As wind farms, solar plants, and ESSs are considered, the proposed DEOC will only act upon CCs connected to particular buses, located within the grid based on energy potential or technical considerations. However, in an initial exploratory aim to account for full controllability, this paper assumes controllable components deployed at all non-generator buses. In future research, this assumption will not be required.

### A. 9-bus system

A self-cleared three-phase fault is applied at bus 8 with a total duration of 150 ms. The system dynamics are dominated by two electromechanical modes: one oscillation between G1 (slack bus) and G2-G3 with a corresponding eigenvalue  $\lambda_1 = j7.35$  (1.17 Hz), and another between G2 and G3 with a corresponding eigenvalue  $\lambda_2 = j13.69$  (2.18 Hz). The fault

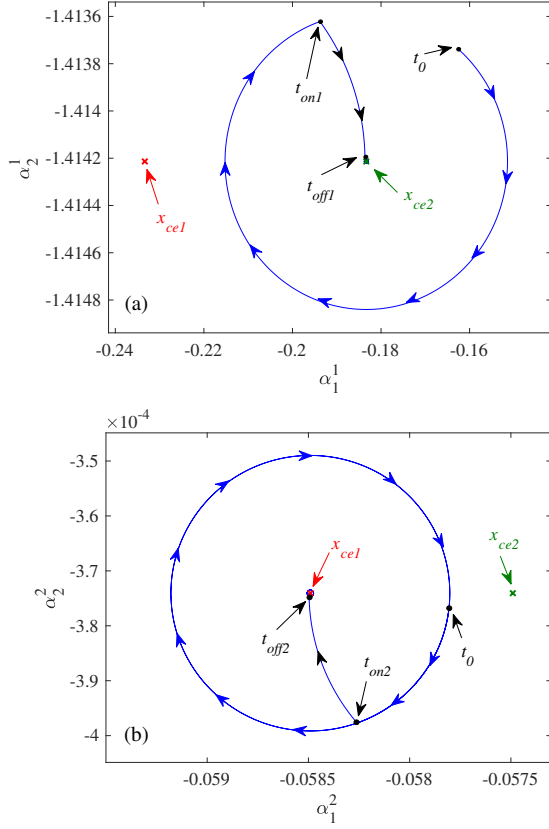


Fig. 3. 9-bus system projected dynamics: (a) projection into the  $\alpha$ -plane related to the 1.17 Hz mode (first tackled mode), (b) projection into the  $\alpha$ -plane related to the 2.18 Hz mode (second tackled mode).

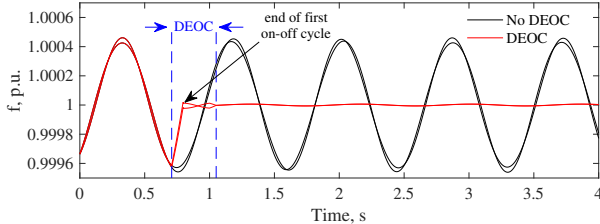


Fig. 4. 9-bus system frequency dynamics.

at bus 8 mostly excites the 1.17 Hz mode. Because of this, the DEOC is performed first to tackle that specific mode. In order to do so, the equilibrium point is shifted only on the projected subspace related to that mode (see Fig. 3-(a)).

By using the switching function defined in eq. (17), the switch-on time is  $t_{on1} = 0.708$  s. Next, every time step after  $t_{on1}$ , the integral of  $E_k(t)$  is computed over a moving time window with a width of  $T = 1$  s. When the first minimum is found, the switch-off is activated; this is at  $t_{off1} = 0.796$  s. A minimum integral denotes that the oscillation is close to the original equilibrium point, thus the oscillation associated with this mode is almost annihilated. Note that after the annihilation of this oscillation, the system is dominated exclusively by the 2.18 Hz mode. As mentioned before, this mode corresponds to

an oscillation between G2 and G3. From Fig. 4 it is noticeable that just after this first on-off cycle, both SG frequencies are in counter-phase.

Then, the targeted mode is changed to the one with a frequency of 2.18 Hz. Now, it is desired to shift the equilibrium point only on the subspace associated with this mode. As shown in Fig. 3-(b), the controlled orbit centered at  $x_{ce2}$  does not induce any displacement on the already tackled 1.17 Hz mode. Next, the second switchings are at  $t_{on2} = 1.000$  s and  $t_{off2} = 1.051$  s. With this second operation, a sub-optimal annihilation of both modes is performed. Even though both modes are not completely eliminated, the SGs frequency time evolution shown in Fig. 4 validates the performance of the DEOC with a reduction of oscillation amplitude greater than 95% in both modes. The total actuation of the DEOC is 0.343 s. Note that in a practical operation scenario, SG dampers and PSSs would take care of the remaining oscillation.

### B. 39-bus system

A self-cleared three-phase short-circuit is considered at bus 9 with a total duration of 150 ms. In a real setup, online measurement and oscillation identification techniques can be used to determine the most dominant modes, which will be targeted with a given order. In this simulation, the order is defined as shown in Table I, based on the amplitude of each excited mode. A moving time window with a width of  $T = 1$  s is considered to compute the integral of  $E_k(t)$ .

TABLE I  
39-BUS SYSTEM MODES AND DEOC SWITCHING TIMES

Mode	Frequency (Hz)	DEOC order	$t_{on}$ (s)	$t_{off}$ (s)
1	0.62	1	0.607	0.807
2	1.53	2	1.456	1.611
3	2.52	3	1.668	1.756
4	1.75	4	2.199	2.286
5	1.72	5	2.823	2.887
6	2.83	-	-	-
7	2.75	-	-	-
8	2.37	-	-	-
9	1.29	-	-	-

Simulation results are shown in Fig. 5, where the speed of all SGs is compared with the case without DEOC. Fig. 5-(a) shows the DEOC application when the switching function derived in equation (17) is used. Even though, this function ensures that the original equilibrium point  $x_e$  belongs to the controlled trajectory, it does not give a specific time when this is going to happen. In a multi-mode system, this optimal time may exceed an expected time for control purposes. Consequently, only a sub-optimal solution is found in a short time to perform each switch-off. Because of this, a complete annihilation of each dominant mode cannot be achieved within a reasonable time frame for this system.

However, a local search is done around the switch-on time to shed light on this issue. After a few tries, adequate switch-on times have been found that almost annihilate the oscillations. The result is shown in Fig. 5-(b) using the following adjusted

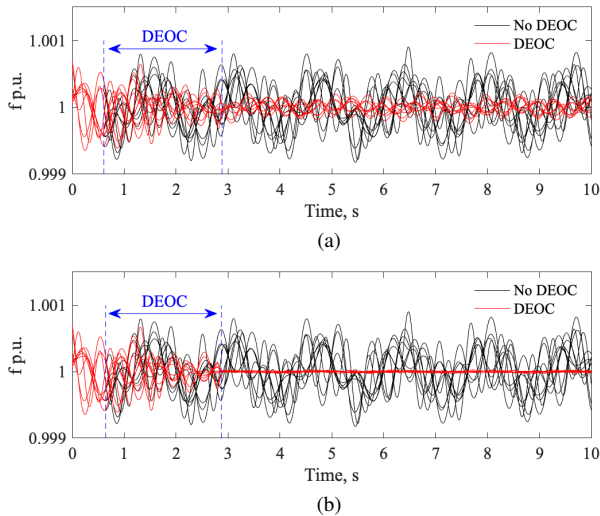


Fig. 5. 39-bus system dynamics: (a) sub-optimal solution by using  $h(x) = 0$ , (b) optimal solution by ensuring  $x_e$  belongs to the controlled trajectory in an adequate time to switch off.

switch-on times for the 5 targeted modes: 0.642, 1.497, 1.678, 2.165, and 2.800 s. The authors recognize that further exploration is needed to acquire a formal theoretical foundation to guarantee this condition. An additional time-dependent constraint to the switching function  $h(x)$  might suffice to improve the DEOC performance. The remaining oscillations after the DEOC are in essence the initially exciting modes that are not tackled. This result validates the effectiveness of the proposed control and its application to handle a large-scale system with a multi-mode dynamic nature. A total oscillation amplitude reduction greater than 90% of all five dominant modes is achieved.

#### IV. CONCLUSION

This paper presents significant advances in the discrete electromechanical oscillation control problem. The DEOC aims to incorporate EIRs into the control of the dynamic response of the system. These controllable components are considered to provide step-wise changes in their power output to transiently shift the system equilibrium point. By doing so, the oscillations of dominant excited modes are proposed to be progressively annihilated. Orthogonal projections are used to define the required power output of every CC. A switching function is derived to define the switch-on time. In the same way, the integral of the oscillation energy is used as a merit function to establish the switch-off time. The incorporation of the DEOC is validated in a 9-bus and a 39-bus systems. To fully explore the theoretical implications of CC locations, a CC is assumed to be connected to every non-generator bus. Simulation results are categorical: the oscillation amplitude of dominant modes is significantly reduced (greater than 90%) with a short time of DEOC actuation ( $<2.3$  s). These results reveal that the proposed approach can handle large-scale systems, with multi-mode dynamics. The next step in

developing this control technique is to achieve similar results only considering a subset of non-generator buses.

#### REFERENCES

- [1] B. Kroposki, "Integrating high level of variable renewable energy into electric power systems (NREL-PR-5D00-68349)," Power Systems Engineering Center, National Renewable Energy Lab., Tech. Rep., 2018.
- [2] N. Nguyen and J. Mitra, "An analysis of the effects and dependency of wind power penetration on system frequency regulation," *IEEE Transactions on Sustainable Energy*, vol. 7, no. 1, pp. 354–363, 2016.
- [3] J. Slootweg and W. Kling, "The impact of large scale wind power generation on power system oscillations," *Electric Power System Research*, vol. 67, no. 1, pp. 9–20, 2003.
- [4] M. Aboul-Ela, A. Sallam, J. McCalley, and A. Fouad, "Damping controller design for power system oscillations using global signals," *IEEE Transactions on Power Systems*, vol. 11, no. 2, pp. 767–773, 1996.
- [5] D. Vowles, C. Samarasinghe, M. Gibbard, and G. Ancell, "Effect of wind generation on small-signal stability — a new zealand example," in *2008 IEEE Power and Energy Society General Meeting - Conversion and Delivery of Electrical Energy in the 21st Century*, 2008, pp. 1–8.
- [6] C.-L. Chang and S. Maharjan, "Analysis of damping oscillation using discrete control signals from phasor measurement unit (pmu)," in *2015 North American Power Symposium (NAPS)*, 2015, pp. 1–5.
- [7] H. Silva-Saravia, H. Pulgar-Painemal, and J. M. Mauricio, "Flywheel energy storage model, control and location for improving stability: The chilean case," *IEEE Transactions on Power Systems*, vol. 32, no. 4, pp. 3111–3119, 2017.
- [8] D. Cai, P. Wall, M. Osborne, and V. Terzija, "Roadmap for the deployment of wampac in the future gb power system," *IET Generation, Transmission & Distribution*, vol. 10, no. 7, pp. 1553–1562, 2016.
- [9] H. Zhang, "Peak Reliability synchrophasor technology roadmap for control room solution," Peak Reliability, EMS Network Apps. Manager. RC User Group Meeting, Denver, CO, USA, Tech. Rep., 2017.
- [10] D. K. Reitan and N. RamaRao, "A method of improving transient stability by bang-bang control of tie-line reactance," *IEEE Trans. on Power Apparatus and Systems*, vol. PAS-93, no. 1, pp. 303–311, 1974.
- [11] N. P. Johansson, H.-P. Nee, and L. Angquist, "Discrete open loop control for power oscillation damping utilizing variable series reactance facts devices," in *Proceedings of the 41st International Universities Power Engineering Conference*, vol. 2. IEEE, 2006, pp. 785–789.
- [12] N. Ratmarao and D. K. Reitan, "Improvement of power system transient stability using optimal control: Bang-bang control of reactance," *IEEE Transactions on Power Apparatus and Systems*, vol. PAS-89, no. 5, pp. 975–984, 1970.
- [13] D. Kosterev and W. Kolodziej, "Bang-bang series capacitor transient stability control," *IEEE Transactions on Power Systems*, vol. 10, no. 2, pp. 915–924, 1995.
- [14] J. Chang and J. Chow, "Time-optimal series capacitor control for damping interarea modes in interconnected power systems," *IEEE Transactions on Power Systems*, vol. 12, no. 1, pp. 215–221, 1997.
- [15] H. Pulgar-Painemal and S. Martinez-Lizana, "On the search for expanded grid control capabilities: Discrete control on emerging power technologies," *arXiv:2209.06239 [eess.SY]*, 2022.
- [16] H. Silva-Saravia, Y. Wang, H. Pulgar-Painemal, and K. Tomsovic, "Oscillation energy based sensitivity analysis and control for multi-mode oscillation systems," in *2018 IEEE Power Energy Society General Meeting (PESGM)*, 2018, pp. 1–5.
- [17] H. Silva-Saravia, H. Pulgar-Painemal, D. A. Schoenwald, and W. Ju, "Adaptive coordination of damping controllers for enhanced power system stability," *IEEE Open Access Journal of Power and Energy*, vol. 7, pp. 265–275, 2020.
- [18] R. D. Zimmerman, C. E. Murillo-Sánchez, and R. J. Thomas, "Matpower: Steady-state operations, planning, and analysis tools for power systems research and education," *IEEE Transactions on Power Systems*, vol. 26, no. 1, pp. 12–19, 2011.